Dose mapping a gamma-ray irradiator and x-ray irradiator to obtain rodent absorbed depth dose equivalence between technologies

Robin Peter[1,2], Javier Caravaca[1], Jaewon Yang[3], Chad Gunther[4], Juan Antonio Camara Serrano[5], Christopher Nostrand[4], Veronica Steri[5], and Youngho Seo[1,2]

[1]*Physics Research Laboratory, University of California, San Francisco, USA*
[2]*Department of Nuclear Engineering, University of California, Berkeley, USA*
[3]*Department of Radiology, University of Texas Southwestern Medical Center, Dallas, Texas, USA*
[4]*C&C Irradiator Service, LLC, Washington, DC., USA*
[5]*Helen Diller Family Comprehensive Cancer Center, University of California, San Francisco, USA*

Abstract

The National Nuclear Security Administration (NNSA) Office of Radiological Security (ORS) is implementing a radiological risk reduction program promoting the use of non-radioisotopic technologies in a range of applications, including blood and research irradiation. In support of this aim, and to assist in the transition from gamma-ray to x-ray based irradiation, ORS funds studies which examine the efficacy of x-ray irradiation compared to gamma-ray irradiation. Traditionally, gamma-emitter ^{137}Cs has been used to study the biological effects of radiation in small animals. To determine the feasibility of replacement with x-ray irradiators in this application, ORS funded the University of California San Francisco (UCSF) and C&C Irradiators to compare the rodent absorbed dose rates from a gamma-ray irradiator to an x-ray irradiator using the same dosimetry techniques on each device. Conventional x-ray irradiators produce polychromatic x-ray spectra that are typically less penetrative than ^{137}Cs gamma rays and yield different spatial distributions of dose in anatomical structures. However, careful device calibration can be used to plan dose to specific tissue types, allowing for controlled use of x-ray irradiators in place of ^{137}Cs irradiators. This study compares direct dose measurements in 3D-printed rodent mouse phantoms and Monte Carlo simulations of the MOBY-4 mouse model to quantify the total and organ-specific dose delivered by each technique and establish a dosimetry system for researchers which can be translated from gamma- to x-ray irradiators. This work advances scientific knowledge towards the use of x-ray in place of gamma-ray irradiation in the biomedical research community, and ultimately advocates a more responsible use of radioactive-related technologies for a safer world.

1. Introduction

The National Nuclear Security Administration Office of Radiological Security (NNSA/ORS) has developed a radiological risk reduction program to reduce the use of high activity radiological sources in hospitals and research settings by replacement with non-radioisotopic technologies [1]. To support these aims and assist in the transition from gamma-ray to x-ray based irradiation, ORS funds studies which examine the efficacy of x-ray irradiation compared to gamma-ray irradiation in a range of applications.

Traditionally, gamma-emitter ^{137}Cs has been used to study the biological effects of radiation in humans using small animal models; however ^{137}Cs irradiation devices use high-activity dispersible cesium chloride sources that pose safety and security risks. Replacement with non-radioisotopic alternatives such as x-ray would eliminate these hazards and reduce the need for strict deployment and utilization controls in irradiation experiments. To determine the feasibility of this technological switch, ORS funded the University of California, San Francisco (UCSF) and C&C Irradiator Service, LLC to compare the rodent absorbed dose rates from a ^{137}Cs gamma-ray irradiator and those from an x-ray irradiator.

Gamma- and x-ray irradiation have different physical properties and use different delivery systems, which may result in different absorbed dose distributions in tissue. ^{137}Cs decays via two pathways to ^{137}Ba through β^- emission or β^-,γ emission, yielding a monoenergetic gamma-ray of 662keV (85.1%). In comparison, commercial x-ray irradiators produce polyenergetic photon spectra with low- to medium-energy components up to 320 keV. Higher energy photons imply higher penetration and longer-range secondary ionizing radiation (electrons). Additionally, the technological complexity of x-ray production leads to several systematic considerations not present in most simple gamma-ray irradiators (absolute number of produced photons, energy distribution, angular distribution, etc.).

Existing work to quantify the effects of these factors on biological endpoints have focused mainly on bone marrow [2–7]. And while dose calibration protocols are well-defined in the clinical setting, lack of machine-specific calibration requirements in preclinical studies can lead to dramatic variance of delivered dose between research settings [8] (one study found up to 42% output difference between machines across 12 radiation biology laboratories) [9]. Existing procedures to calibrate x- and gamma-ray irradiators, when used, both do not account for the anatomical complexity of the subject.

This work aims to fill this gap by providing a comprehensive comparison study of dose in mice between a ^{137}Cs irradiator (Mark I-68) and an x-ray irradiator (X-Rad320). We use experimental data and a realistic Monte Carlo simulation to assess dose equivalence and discrepancies between the two and demonstrate an *in situ* dose calibration technique based on 3D-printed biophantoms to verify and calibrate machine output.

2. Methods

The absolute dose delivered by each irradiator is measured for four machine outputs (160 kVp x-rays, 225 kVp x-rays, 320 kVp x-rays, and 662 keV gamma-rays) in mouse carcasses and 3D-printed rodent biophantoms (RBPs) implanted with alanine dosimeters. Each system and subject is built in a custom Monte Carlo (MC) framework, calibrated with an in situ alanine cassette measurement, that calculates voxel-specific dose and dose rate in a digital mouse phantom for each of the experimental irradiations. The detailed simulation allows estimation of organ-specific absorbed doses for each irradiation and helps delineate the effect on absorbed dose due to specific experimental factors, including photon energy spectra, beam delivery geometry and radiation distribution, and subject position and anatomy. Validation of the 3D-RBP dose measurements with the real mouse carcasses provides a direct *in situ* calibration procedure.

2.1 Irradiators

The Mark I-68 (JL Shepherd and Associates, San Fernando, CA) is selected in this study as a representative ^{137}Cs gamma-ray irradiator for small animal biomedical research [10, 11]. Its

interior cavity is shielded by lead and contains a rotating turntable and a source guide to translate an active cesium chloride source into position to irradiate the subject. In this study, two colinear source cylinders were used, totaling 2068 Ci at the time of experiment (June 22, 2021).

The X-Rad320 is used as a representative x-ray irradiator in this study, featuring a self-shielded cabinet that houses an adjustable subject positioning shelf and an x-ray tube with capabilities up to 320 kVp/12.5 mA. A hard F2 thoraeus filter (1.5 mm Al + 0.25 mm Cu + 0.75 mm Sn) is included in these experiments.

2.2 Subjects

Each mouse carcass is implanted with three parafilm-wrapped alanine pellets, provided by the National Institute Standards and Technology (NIST) via Far West Technology, inside the cranium, thoracic cavity, and subdermal pelvic area. Following irradiation, the alanine pellets are removed and measured by NIST in their electron paramagnetic resonance (EPR) facility according to standard protocols.

Three types of RBPs are fabricated using combinations of polylactic Acid (PLA+), thermoplastic elastomer (TPE), acrylonitrile butadiene styrene (ABS), and epoxy resin. Bare alanine pellets are implanted in similar locations and measured using the same protocols following subject irradiation.

A Dose-Map™ is used for dose calibration of the Monte Carlo simulation. It consists of 10 μm of Gafchromic MD-V3 film sandwiched between 125 μm layers of matte-polyester substrates, all contained within a high-density polyethylene cassette phantom. An alanine pellet is inserted in the center of the phantom for absolute calibration against NIST standards. Fig. 1 shows the Dose-Maps™ positioned in each irradiator and the printing process for the RBPs.

2.3 Irradiation Procedures

A mouse carcass and three RBPs are arranged in a plastic pie cage deployed at the geometric center of each irradiator. The exposure time, beam voltage, current, and source-to-surface distance (SSD) are defined for each irradiation program according to system manufacturer procedures. In total, four runs (160 kVp x-rays, 225 kVp x-rays, 320 kVp x-rays, and 662 keV gamma-rays) irradiated four carcasses and twelve RBPs, each with three alanine dosimeters measured by NIST EPR.

The Dose-Map™ is irradiated separately in each device with the plane of the film positioned perpendicular to the main axis of each beam. Following irradiation, the DoseMaps™ are returned to Ashland™ for measurement. The co-irradiated alanine pellet located at the center is measured by NIST EPR to provide an absolute dosimetry reference.

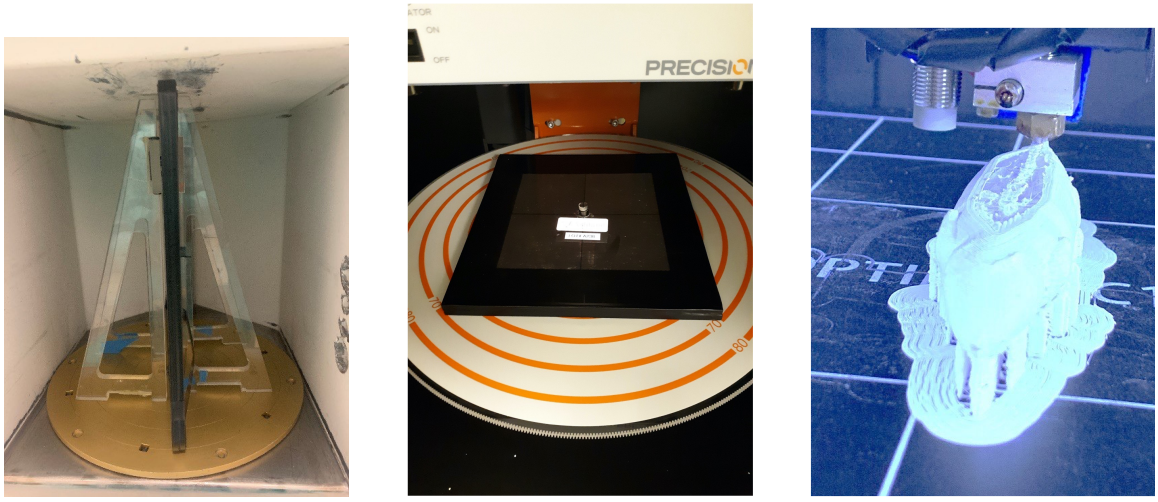

Figure 1: (Left) Inside cavity of Mark I-68 showing turntable geometry and Dose-Map™ film for MC calibration. (Center) Inside cavity of of X-Rad320 showing shelf positioning coordinates and Dose-Map™ film. (Right) 3-D printing process to create RBP.

2.4 Monte Carlo Model

Irradiators and subjects are constructed in a custom GATE (Geant4 Application for Tomographic Emission [12]) model using the Low Energy Livermore physics list. Both irradiators are simulated as air volumes surrounded by lead shielding. Simple geometric shapes (cylinders, rectangular prisms, and pentagonal prisms) are used to build the chamber cavities, DoseMap™, and ^{137}Cs source and source guide. The contributions of plastic supports, copper turntables, and shelving are assumed to be minimal and not explicitly modelled.

Mark I-68: The consistent turntable rotation of this device is modelled as uniform exposure to the subject from all azimuthal angles in one-second time slices. 3.6e10 gamma-rays from ^{137}Cs are simulated, and the results are normalized to the number of generated gamma-rays delivered by the source activity and experimental exposure.

X-Rad320: The x-ray generator is modelled as a directional point source, with energy and angular distributions calculated using SpekPy [13], a Python tool that accounts for the voltage potential, filters, and x-ray extraction angle of the system. 4e10 photons were simulated for each run, and the results are normalized to the experimental number of generated photons delivered by the voltage, tube current, and exposure.

Digital Mouse Phantom: Mouse carcasses are simulated using the digital mouse phantom MOBY [14], custom simplified from 78 materials to 15 relevant organs. The MOBY phantom is modelled inside a realistic polycarbonate plastic pie cage at the center of each cavity. The absorbed dose in each organ is defined as the sum dose of all voxels that belong to that organ.

3. Results and Discussion

Fig. 2 summarizes the following analyses.

3.1 Dose Delivery Accuracy

Each irradiation procedure configured to deliver 25 Gy target dose according to manufacturer specifications. Across three runs (160 kVp, 225 kVp, 320 kVp), the X-Rad320 delivered average absorbed dose to between 14% and 35% of the 25 Gy target. The Mark I-68 (662 keV) delivered more accurate average dose, between -4% and -9% of 25 Gy.

3.2 RBP Dosimetry Accuracy

The RBPs were found to be good surrogates for carcass dosimetry. Over all energies, phantoms, and locations, the average absorbed dose percentage error between RBPs and carcasses was 0.82% ± 5.4%.

3.3 Monte Carlo Validation

Dose-Map™ measurements are compared to MC-simulated dose distributions to provide a correction factor $f = D_m/D_s$, where D_m and D_s are the measured and simulated central doses. Across the four runs (three X-Rad320 and one Mark I-68), correction factors were near unity, averaging $f = 1.06 \pm 0.03$. This result indicates that the MC model adequately accounts for most first-order dose-affecting factors, including photon energy, beam delivery geometry and radiation distribution, and subject position and anatomy. The heel effect is not precisely modelled in the MC framework, so that some geometry asymmetry was observed in experiment that did not appear in simulations.

3.4 Digital Mouse Phantom Dosimetry

The validated MC simulation is used to estimate organ-scale dosimetry of carcass measurements. Our results show that dose uniformity increases with photon energy, reflecting the higher penetration and larger secondary particle range of more energetic photons.

In the MC estimation, soft-tissue organs received fairly uniform dose in all irradiation programs, with higher energy irradiation providing higher uniformity. The standard deviation amongst soft-tissue organs for 160 kVp, 225 kVp, 320 kVp, and 662 keV was 5.2%, 4.9%, 4.7%, 1.7%. However, while dose estimates to bone are similar to soft tissue during ^{137}Cs irradiation, x-ray irradiation programs are predicted to deliver up to double the soft tissue dose to bone. Higher-energy programs are less susceptible to this discrepancy (within 40% percentage error at 320 kVp). Simulated Mark I-68 irradiation is also observed to be more aligned with the target dose in each organ, while the X-Rad320 simulations predict overdosage similar to that observed experimentally.

The discrepancy between bone and soft tissue dose in x-ray irradiation procedures can be understood through photon energy. Higher energy sources, such as 662 keV gamma rays, contribute long-range secondary electrons that deposit a washed-out energy profile along centimeter-scale tracks. Lower energy sources, especially polyenergetic spectra with low energy components, are more likely to be fully absorbed in high-Z structures and thus yield

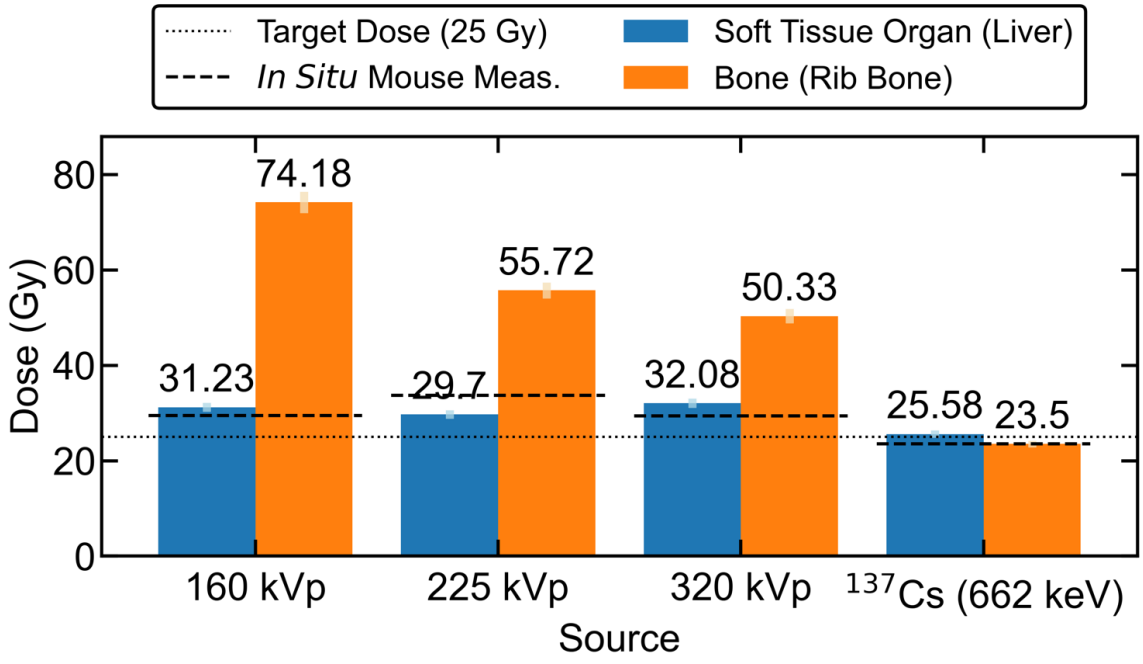

Figure 2: Dosimetry comparison between soft tissue and bone from two of the fifteen simulated organs and tissues for each radiation source, with in situ measurements and target dose (25 Gy) shown. In situ uncertainties are on the order of line widths. X-Rad320 showed more deviation from target dose than Mark I-68, especially in bone, suggesting that calibration (e.g. with RBPs and MC) should be used.

an unequal dose distribution preferential towards bone. This is an important effect that must be accounted for if a precise skeletal bone dose estimate is required. MC simulations like those demonstrated here can be used for this estimation.

3.5 Dose Rate

Dose rates were calculated for each delivery system and run. The highest dose rate is used in the Mark I-68, while the fastest x-ray modality used (X-Rad320 at 320 kVp) delivers dose about 40% slower. The biological implications of these differences is out of the scope of this paper but should be considered in future studies, given a mounting body of work demonstrating the link between dose rate and radiobiological effect [15–19].

4. Summary

We measured the dose delivered in mice using the Mark I-68 Cs-137 irradiator (662 keV) and the X-Rad 320 x-ray irradiator at three different voltages (160 kVp, 225 kVp, and 320 kVp) using mouse carcasses implanted with alanine pellets. Organ-specific doses were estimated using a MC model, validated within 15% at all energies in soft-tissue measurements. The whole-body total absorbed dose does not reflect dose differences between organs due to density, composition, and structure.

Our results show that x-ray irradiation can deliver a similar dose distribution for soft-tissue as ^{137}Cs irradiation. However, elevated bone doses due to lower-energy photon

interactions require careful consideration. MC simulation can be used to estimate bone dose and design a machine protocol to deliver a specific bone or tissue dose. The differences in dose rate and dose distribution between x-ray and ^{137}Cs modalities can also be reduced by using higher-energy x-ray irradiation programs (320 kVp). We, and others, have found significant deviation between target and irradiated dose (35% for X-Rad 320, -9% for Mark I-68). RBPs can provide a soft-tissue *in situ* calibration measurement to calibrate the machine output against this discrepancy and maintain reproducibility across studies.

5. Acknowledgements

This work was supported by the National Nuclear Security Administration of the U.S. Department of Energy and funded through Sandia National Laboratories. All authors declare that they have no known conflicts of interest in terms of competing financial interests or personal relationships that could have an influence or are relevant to the work reported in this paper.

6. References

1. Council, N. R. *et al. Radiation source use and replacement: abbreviated version* (National Academies Press, 2008).
2. Scott, B., Gott, K., Potter, C. & Wilder, J. A comparison of in vivo cellular responses to Cs-137 gamma rays and 320-kV X rays. *Dose-Response* **11,** dose–response (2013).
3. Scott, B. & Potter, C. Stochastic threshold exponential (TE) model for hematopoietic tissue reconstitution deficit after radiation damage. *Dose-Response* **12,** dose–response (2014).
4. Gibson, B. W. *et al.* Comparison of cesium-137 and X-ray irradiators by using bone marrow transplant reconstitution in C57BL/6J mice. *Comparative medicine* **65,** 165–172 (2015).
5. Gott, K. M. *et al.* A comparison of Cs-137 γ rays and 320-kV X-rays in a mouse bone marrow transplantation model. *Dose-Response* **18,** 1559325820916572 (2020).
6. Andersen, A. H. F. *et al.* Comparable human reconstitution following Cesium-137 versus X-ray irradiation preconditioning in immunodeficient NOG mice. *Plos one* **15,** e0241375 (2020).
7. Wittenborn, T. R. *et al.* Comparison of gamma and x-ray irradiation for myeloablation and establishment of normal and autoimmune syngeneic bone marrow chimeras. *Plos one* **16,** e0247501 (2021).
8. Biglin, E. R. *et al.* Preclinical dosimetry: exploring the use of small animal phantoms. *Radiation Oncology* **14,** 1–10 (2019).
9. Pedersen, K. H., Kunugi, K. A., Hammer, C. G., Culberson, W. S. & DeWerd, L. A. Radiation biology irradiator dose verification survey. *Radiation Research* **185,** 163–168 (2016).
10. Brady, S. L., Toncheva, G., Dewhirst, M. W. & Yoshizumi, T. T. Characterization of a Cs-137 irradiator from a new perspective with modern dosimetric tools. *Health physics* **97,** 195–205. issn: 0017-9078 (Sept. 2009).

11. Brodin, N. P., Chen, Y., Yaparpalvi, R., Guha, C. & Tom´e, W. A. Dosimetry Formalism and Implementation of a Homogenous Irradiation Protocol to Improve the Accuracy of Small Animal Whole-Body Irradiation Using a 137Cs Irradiator. *Health Physics* **110,** S26–38. issn: 1538-5159 (Feb. 2016).

12. Sarrut, D. *et al.* Advanced Monte Carlo simulations of emission tomography imaging systems with GATE. *Physics in Medicine & Biology* **66,** 10TR03 (2021).

13. Bujila, R., Omar, A. & Poludniowski, G. A validation of SpekPy: A software toolkit for modelling X-ray tube spectra. *Physica Medica* **75,** 44–54 (2020).

14. Segars, W. P. & Tsui, B. M. MCAT to XCAT: The evolution of 4-D computerized phantoms for imaging research. *Proceedings of the IEEE* **97,** 1954–1968 (2009).

15. Hall, E. J. & Brenner, D. J. The dose-rate effect revisited: radiobiological considerations of importance in radiotherapy. *International Journal of Radiation Oncology* Biology* Physics* **21,** 1403–1414 (1991).

16. Rühm, W. *et al.* Dose-rate effects in radiation biology and radiation protection. *Annals of the ICRP* **45,** 262–279 (2016).

17. Brooks, A. L., Hoel, D. G. & Preston, R. J. The role of dose rate in radiation cancer risk: evaluating the effect of dose rate at the molecular, cellular and tissue levels using key events in critical pathways following exposure to low LET radiation. *International journal of radiation biology* **92,** 405–426 (2016).

18. Down, J., Tarbell, N., Thames, H. & Mauch, P. Syngeneic and allogeneic bone marrow engraftment after total body irradiation: dependence on dose, dose rate, and fractionation. *Blood* **77,** 661–669. issn: 0006-4971. eprint: https://ashpublications.org/blood/ article-pdf/77/3/661/604651/661.pdf. https://doi.org/10.1182/blood.V77. 3.661.661 (Feb. 1991).

19. Paunesku, T., Stevanović, A., Popović, J. & Woloschak, G. E. Effects of low dose and low dose rate low linear energy transfer radiation on animals–review of recent studies relevant for carcinogenesis. *International Journal of Radiation Biology* **97,** 757–768 (2021).